

Received September 17, 2021, accepted October 2, 2021, date of publication October 6, 2021, date of current version October 14, 2021.

Digital Object Identifier 10.1109/ACCESS.2021.3118281

RobHand: A Hand Exoskeleton With Real-Time EMG-Driven Embedded Control. Quantifying Hand Gesture Recognition Delays for Bilateral Rehabilitation

ANA CISNAL¹, (Student Member, IEEE), JAVIER PÉREZ-TURIEL¹, JUAN-CARLOS FRAILE¹, DAVID SIERRA¹, AND EUSEBIO DE LA FUENTE

Instituto de las Tecnologías Avanzadas de la Producción (ITAP), University of Valladolid, 47011 Valladolid, Spain

Corresponding author: Ana Ciscal (ciscal@ieee.org)

This work was supported in part by a grant from the Spanish Centro para el Desarrollo Tecnológico Industrial (CDTI) under project ROBHAND-IDI 2017 0263, with funds from the European Regional Development Fund (ERDF) and in part by a grant from the Ministerio de Ciencia e Innovación under project RTC2019-007350-1.

ABSTRACT Assisted bilateral rehabilitation has been proven to help patients improve their paretic limb ability and promote motor recovery, especially in upper limbs, after suffering a cerebrovascular accident (ACV). Robotic-assisted bilateral rehabilitation based on sEMG-driven control has been previously addressed in other studies to improve hand mobility; however, low-cost embedded solutions for the real-time bio-cooperative control of robotic rehabilitation platforms are lacking. This paper presents the RobHand (Robot for Hand Rehabilitation) system, which is an exoskeleton that supports EMG-driven assisted bilateral by using a custom-made low-cost EMG real-time embedded solution. A threshold non-pattern recognition EMG-driven control for RobHand has been developed, and it detects hand gestures of the healthy hand and replicates the gesture on the exoskeleton placed on the paretic hand. A preliminary study with ten healthy subjects is conducted to evaluate the performance in reliability, tracking accuracy and response time of the proposed EMG-driven control strategy using the EMG real-time embedded solution, and the findings could be extrapolated to stroke patients. A systematic review has been carried out to compare the results of the study, which present a 97% of overall accuracy for the detection of hand gestures and indicate the adequate time responsiveness of the system.

INDEX TERMS Electromyography, embedded software, exoskeletons, real-time systems, rehabilitation robotics.

I. INTRODUCTION

Cerebrovascular accidents (stroke) are the second leading cause of death worldwide and caused almost 6 million of the 56.9 million deaths worldwide in 2016 according to the World Health Organization (WHO) [1]. Stroke is the third leading cause of disability, and it mainly affects individuals at the peak of their productive life [2]. Approximately, 70 to 80 percent of the stroke survivors require long-term medical care [3] and live with a poor quality of life (QOL) [4], [5].

Approximately 75 % of people suffer some degree of paresis on their upper limbs [6], especially their hands [7]. Individuals who have suffered a chronic stroke often exhibit spasticity in the paretic hand, which leads to a reduction of the hand range of motion (ROM) [8]. Muscle weakness

is also present to varying degrees in the majority of stroke patients [9], [10]. Stroke patients improve hand motor performance by repetitive task practice rehabilitation (RTP), which leads to improvements in the range of motion and hand strength [11].

RTP rehabilitation consists of breaking down a task into individual movements and practicing these exercises continuously, and it involves activities of daily living. However, RTP rehabilitation is costly because it is strenuous labor, and it requires considerable time commitment by both the patient and rehabilitation specialist [12]. A rehabilitation robotic system that allows the patients to perform the repetitive exercise without the continuous assistance of the therapist would make physical therapy more accessible and affordable and would increase the potential for better outcomes [13].

Clinical studies have shown that hand motor reflexes significantly improve when performing intense repetitive

The associate editor coordinating the review of this manuscript and approving it for publication was Liang-Bi Chen¹.

movements assisted by robotic devices [14]–[17], thus indicating the advantage of robotic devices compared to conventional therapies because they facilitate independent rehabilitation with the possible outcome of increasing the training repetitions and patient motivation [18], [19]. For this reason, robotic hand rehabilitation systems have recently been developed a complementary approach to that of traditional therapies.

Effective training paradigms implemented on rehabilitation robots for motor recovery are passive, assistive, active-assistive, active and resistive. In this context, a training paradigm expresses how the robot interacts with the patient considering the subject's status and the applied forces [20]. In the passive training modality the hand motion of the patient only depends on the force applied by the robot, whereas the other paradigms also depend on the intention and/or force applied by the user [20].

Passive rehabilitation usually implements positional control to perform repetitive training, and the robot is only responsible for the movement of the patient's finger. However, in an active-assistive training modality, the robot exerts assisting forces only if the patient intends to perform a movement even if he/she cannot perform the desired movement autonomously.

The passive training modality has been found to be temporarily effective for reducing hypertonia in chronic stroke patients [21] and for maintaining the hand range of motion in the early stage of the treatment; however, it does not significantly improve motor function [22]. Conversely, active-assistive training is more effective for improving motor skills than passive control [22], [23]. However, active-assistive systems implement a more complex control system because the robot needs to detect the user's motion intention.

The most common method for detecting user intention is to measure the contact force, which is usually performed at the fingertips. However, intrinsic problems are observed because the force exerted by the user cannot be distinguished by externally applied forces; thus, user intention cannot be determined [24], [25]. In addition, this technique may obstruct the user's sense of feeling because the force sensors are usually placed on the fingertips. Alternatively, user intention can also be determined from biomechanical signals, such as electromyography (EMG), encephalography (EEG), mechanomyography, photoplethysmography at fingernails or finger pad deformations [26].

sEMG-based control strategies have been proposed for hand rehabilitation robot control because the user motor intention can be inferred from EMG activity detected with skin surface electrodes. Another advantage is the inherent property of the EMG signals because the electromechanical latency or delay (ED) of the EMG signals (time interval from the onset of the EMG signal to the onset of force production during a muscle contraction) is approximately 10–300 ms [27], [28], which reduces the system latency, thus allowing for a more natural human-robot interaction (HRI).

The first proposed sEMG control strategies were the so-called binary control [29], which is also known as ON-OFF control [30], EMG-triggered control [31] or threshold control strategies [32], [33]. Currently, non-pattern recognition methods underlie most of the EMG implemented controls because of their simplicity and good results. However, the implementation of pattern recognition-based control methods, such as fuzzy logic controls [34]–[36], artificial neural networks [37]–[40], support vector machines (SVM) [41], [42] and linear discriminant analysis (LDA) [43], [44], has experienced substantial growth in recent years because these classification algorithms can be used to accurately determine different hand gestures.

The advantage of using classifier algorithms and pattern recognition instead of non-pattern recognition methods is the possibility of determining numerous predefined hand gestures, which allows for complete and accurate position control because different types of grasping can be distinguished. However, determining multiple types of grasping requires numerous electrodes [45]–[51], and most of the sEMG-based pattern recognition techniques proposed in the literature are not applicable in practical cases because they require a hand exoskeleton with a large number of DoFs and high computational requirements, which cannot be supported by real-time embedded systems [52], [53].

Bilateral therapy, which is based on replicating the reference motion that produces the healthy hand in the exoskeleton attached to the impaired hand, can be achieved by implementing an EMG-driven control (also called self-motion control [54]). Bilateral training follows the same principles of mirror therapy, which consists of placing a mirror in front of the patient in a way that the reflection of the healthy hand in the mirror creates an illusion that the affected limb is being moved. The only difference with bilateral training is that the illusion provided by the mirror is replaced by the real motion of the paretic limb because of the assistance of the hand exoskeleton. Traditional mirror therapy has been widely used for many years because of its usefulness in motor recovery [55], [56]. In recent years, bilateral robotic training has gained popularity [54], [57], [58].

After a stroke, paretic limbs usually suffer muscle spasticity and weakness, mostly in the first weeks after the episode [59]. Usually, flexors have more spasticity while extensors suffer more weakness [60]. Because muscle activity of the impaired hand is often unreliable after a stroke due to spasticity or flaccidity, driving the exoskeleton from the healthy hand activity in bilateral training has especially great potential.

In this paper, a low-cost real-time embedded EMG-driven robotic hand exoskeleton for bilateral rehabilitation is presented. The RobHand project aims to develop a robotic rehabilitation device designed to help stroke survivors improve the range of motion, strength and motor function of the hand, which can subsequently reduce impairment and improve their quality of life.

TABLE 1. Selected EMG-driven hand rehabilitation robots.

Ref	EMG acquisition system	Platform for EMG control	Control type	Acc ⁽¹⁾	Delay ⁽²⁾
[53]	Myoware Muscle Sensor (Advanced Technologies)	PC	Point-in-Polygon	yes	no
[57]	g.USBamp amplifier (g.tec)	PC	Neural network	yes	no
[68]	e-Health Sensor Shield (Cooking hacks)	Arduino-based controller	Threshold algorithm	no	no
[69]	Bagnoli-8 EMG System (Delsys) and USB-6221 data acquisition device (National Instruments)	PC	Linear Bayes classifier	yes	yes
[70]	MyoArmband (Thalmic Labs)	PC	Classification algorithm	yes	yes
[71]	MyoArmband (Thalmic Labs)	Not specified	Inference method	no	no
[72]	Trigno wireless EMG system (Delsys)	Not specified	Neural network	no	no
[73]	MyoArmband (Thalmic Labs)	Not specified	Forest classifier	yes	no
[74]	Cyton (OpenBCI)	PC	Neural network	yes	no

⁽¹⁾ Whether information about accuracy of the EMG control is provided. ⁽²⁾ Whether delay analysis of the system is carried out.

The RobHand rehabilitation robotic system may be used as a complement for manual therapy because traditional rehabilitation programs are time-consuming and labor-intensive. Furthermore, there is a need to facilitate home-based rehabilitation because post-stroke programs typically consist of 3-one-hour sessions per week, which end 6 months after the incident [61]. Consequently, RobHand should be applicable in clinical and home settings, and must be fully portable, compact and lightweight as well as cost affordable and easy to operate.

The main challenge is the implementation of an affordable and compact rehabilitation platform for home environments, which necessarily implies the integration of low-cost technological solutions and safe and intensive training. Bio-cooperative control integrate psycho-physiological information into the control loop [62]. The implementation of this kind of control in robots usually requires the installation of expensive physiological acquisitions systems, and their high cost limits the availability of these therapies [63]. The RobHand rehabilitation system aims to provide a low-cost bio-cooperative control system based on EMG; therefore, designing and developing a low-cost EMG acquisition device is mandatory.

Currently, the number of EMG embedded implementations are relatively limited. Some examples are the projects by Benatti *et al.* [47], [64], the Johns Hopkins University Applied Physics Laboratory [65], Liu *et al.* [66] and Brunelli *et al.* [67]. In addition, there are very few works in the literature related to hand rehabilitation exoskeletons using EMG-driven control where the complete robotic system is addressed (see Table 1).

As shown in Table 1, most proposals use high-cost commercial EMG signal acquisition systems (only [53] uses low-cost EMG sensors that cost less than 150€) and the exoskeleton control is normally run on a PC or the platform is not specified (only [68] runs the control using an embedded controller). Therefore, to our knowledge, no exoskeleton for hand rehabilitation includes both a low-cost signal acquisition system and performs real-time control through an embedded platform. Furthermore, little or no information about latency of the system is provided (only in [69] and [70]). Both accuracy and latency are highly critical for guaranteeing a natural

and reliable human-robot interaction; however, the literature review did not obtain results on these factors (Table 1).

In this paper, a low-cost and compact solution is presented, and it consists of a microcontroller and an EMG acquisition device, thereby providing an embedded solution for implementing a real-time EMG-driven control for the RobHand exoskeleton.

The EMG-driven control implemented in RobHand is based on a non-pattern recognition method and implements EMG threshold control because its simplicity is appropriate for an embedded system and does not compromise the control accuracy, and it allows for the possibility of using just two pairs of electrodes. This control only allows for the classification of three predefined hand gestures (rest, open, and close). Although the hand can adopt multiples postures, they can be limited to these three without reducing the efficiency of applying robotic rehabilitation to the activities of daily living (ADL) [75]. A preliminary test to evaluate the performance of the proposed EMG-driven control in RobHand is performed, and the accuracy and latency times of the system are calculated in detail.

The cost of the whole rehabilitation system is reduced not only by designing a custom-made EMG acquisition system but also by using compliant low-cost non-backdrivable actuators. The non-backdrivability of the actuators could present a serious disadvantage; however the EMG-driven control allows for bimanual therapy, which indicates that this limitation of the actuators does not influence the mechanical behavior of the rehabilitation robotic platform.

In summary, RobHand implements an active-assistive paradigm using an EMG-driven control to restore the capacity of opening and closing the hand of patients who have suffered a cerebrovascular accident. The proposed EMG-driven control, or self-motion control, allows the patient to perform bilateral therapy, in which the exoskeleton worn on the impaired hand moves according to the recorded sEMG signals of the forearm of the healthy hand.

This paper is organized as follows: an overview of the RobHand exoskeleton hand robotic rehabilitation platform is provided in Section 2, and it details the electromechanical hand module, the embedded electronic system and the EMG-driven control. In Section 3, the EMG-assisted bilateral

rehabilitation is explained in more detail, including the muscle selection and the electrode placement for measuring the EMG signals, the algorithm for EMG signal normalization, the calibration process and the threshold EMG-driven control. The experimental results are presented in Section 4, with a focus on subject selection, the experimental procedure and the variables to measure. A discussion of the obtained results relative to other previous works and a systematic review are carried out in Section 5. Finally, the conclusions are presented in Section 6.

II. ROBHAND: HAND REHABILITATION ROBOTIC PLATFORM

The RobHand robotic rehabilitation platform includes a hand exoskeleton, and electronic embedded system that runs the EMG-driven control and a windows-based PC that supports virtual therapy environments, patient and task data management, and the HMI. However, the description of the PC tasks is beyond the scope of this paper.

A. HAND EXOSKELETON

The RobHand exoskeleton is based in a direct-driven, under-actuated serial four-bar linkage mechanism, which assists flexion and extension of the thumb and the fingers, and it presents a palm-free design [76]. Five linear actuators L12-30-100-6-I (Actuonix Motion Devices Inc., Victoria, BC, Canada), which provide up to 23N, are used to transmit movement to the distal and proximal phalanges of each finger, whose motion is kinematically coupled.

Using linkages simplifies the mechanism and reduces its size and weight but still provides the flexion and extension angles of a healthy human hand [77]. The links transmit the motion of the motor to the rings that link the mechanical structure to the human proximal and medial phalanges. The rings are made of flexible material (Filaflex 82a), thereby improving the ergonomics of the device and allowing being adaptable to different finger sizes. Furthermore, the rings facilitate the donning and doffing procedures compared to other hand exoskeletons found in the literature. The thumb's position is adjustable through a manual mechanism (Noga LC6200 off-the-shelf device), thus providing easy adaptation to different hand sizes. The exoskeleton weighs approximately 600 g. The RobHand exoskeleton is used along with a forearm support to migrate the effects of the forces and torques generated by the weight of the exoskeleton, which could negatively affect the patient (Fig. 1).

B. EMBEDDED ELECTRONIC SYSTEM

The resulting muscular electrical activity (raw EMG signals), which is the superposition of the motor unit action potential (MUAPs) due to muscle contractions, can be acquired by surface electrodes and appropriate conditioning circuitry. A custom-made application-specific integrated circuit (ASIC) has been designed to acquire and perform the pre-treatment of the forearm electromyographic signals, which are recorded by surface electrodes and transmitted to a microcontroller that is configured for real-time



FIGURE 1. RobHand exoskeleton.

processing operations. The microcontroller performs the digital treatment of the signals to develop the EMG-driven control and apply the appropriate control signals to the actuators to move the exoskeleton according to the user's intention.

The presented embedded electronic system aims to overcome some drawbacks found in related previous works: the high cost of the EMG acquisition system, which is a major obstacle to universal access, and the use of a computer as the data processing platform, which can presumably increase the latency time of the whole rehabilitation system. To overcome these disadvantages, the presented solution has the following features: (1) the EMG acquisition system is custom-made and has been designed to minimize costs as much as possible and (2) a microcontroller is included for on-board processing, and it receives the EMG data just after the analog-to-digital conversion and applies the control signal to the actuators immediately after processing the EMG data, which reduces the latency time of the overall system.

In this subsection, a low-cost, compact, embedded solution for real-time hand exoskeleton EMG-driven control is presented. This solution is primarily based on a microcontroller housed in a LAUNCHXL-F28069M board (Texas Instruments, Texas, EEUU), an EMG acquisition system and a motor driver board (Fig. 2), which are detailed in the following paragraphs.

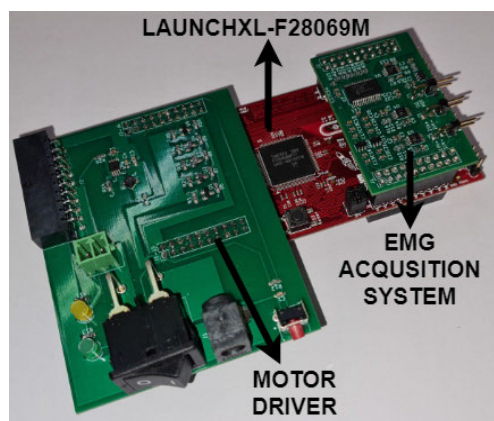


FIGURE 2. LaunchXL-F28069M connected to the motor driver and EMG acquisition system boards.

The real-time microcontroller is a TMS320F28069M (Texas Instruments, Texas, EEUU), which is based on the Harvard architecture and has a 32-bit CPU and a clock speed up to 90 MHz. The embedded memory has 256 KB of Flash, 100 KB of RAM and 2 KB of one-time programmable (OTP) ROM. The TMS320F28069M is included in the F2806x Piccolo™ family of MCUs, which are powered by two coupled cores: C28x core and CLA (Control Law Accelerator). The CLA executes code independently of the C28x core and communicates with it by using a specialized data bus (CLA Bus). This feature will allow the main CPU to be in charge of the communication and the control of the actuators, while the CLA core is only in charge of EMG processing. A large bandwidth of the system will be obtained using this two-core architecture.

A custom 2-channel electromyographic data acquisition ASIC characterized by a 24-bit resolution differential channels and 112 DB of dynamic range (DR) has been designed and developed. Each channel consists of an instrumentation amplifier (gain of 50), followed by an RC low-pass filter (cutoff frequency of 150 Hz). To prevent saturation of the instrumentation amplifier, each channel is designed to compensate differential input offset. The delta-sigma modulator of the analog front end (AFE) is configured to run at a 3.3 MHz frequency, and the oversampling ratio is set to 4096, resulting in each channel being sampled at 200 Hz. The ASIC is designed to interface with the TMS320F28069M MCU via SPI communication and other necessary digital signals to transmit the raw EMG signals. The board is designed on a 4-layer PCB with a single ground plane (inner layer 2) in the analog circuitry and two ground planes (top and bottom) in the digital circuitry, in a way that ground planes are split to separate both analog and digital circuits, while the rest of layers are for signal lines. The board is designed as a booster pack (or shield); therefore, wires are not needed to connect to the LAUNCHXL-F28069M. Discrete components are placed on both top and bottom layers to further reduce the resulting board size, which is 50.8×33 mm. The chip occupies an active area of 10 cm^2 and consumes 3 mW from 3.3 V power supplies.

The hand exoskeleton has five linear actuators, namely, L12-30-100-6-I (Actuonix Motion Devices Inc.), with 30 mm length strokes for moving the MCP and DIP joints of the digits of the hand. The actuators are powered by 6 V DC power, are low-priced, weigh 34 g, have a maximum speed of 25 mm/s and maximum force of 42 N and present very low backdrivability due to the 100:1 gear ratio.

Miniature Linear Motion Series L12-I has an embedded internal position controller that can control the position by using the 0-5 V interface and the PWM mode by applying a 5 V, 1 KHz PWM input signal, whose pulse width is proportional to the desired position or the stroke extension percentage. The actuators are controlled by the TMS320F28069M MCU, which generates 3.3 V PWM output signals; therefore, a motor driver (a bridge between the microcontroller and the actuators) must be designed and developed, and it increases

the voltage level of the PWM output signal from 3.3 to 5 V to meet the specifications of the PWM mode control.

The motor driver board is composed of five drivers to control the five actuators independently. Each motor driver is a voltage-rise circuit, which has an amplification stage mainly composed of an N-channel MOSFET Transistor BSS138. The motor driver board provides a single connector for the five actuators and facilitates the connection of the hand exoskeleton to the electronic box. It also has a reset button for the microcontroller, a 6 V DC jack power connector in series with an on/off switch to connect/disconnect the power and two LEDs to visually indicate the power status of the microcontroller and the power supply. For security reasons, it also has a connector to plug in a custom kill-switch to shut down power to the actuators. The developed motor driver board is a 2-layer PCB that has discrete components only placed on the top layer, and it is also designed as a booster pack to avoid connecting external wires.

The EMG acquisition system and the motor drivers have been designed independently, and as a result, the system is composed of two PCBs because in the first stage of the project, passive control was carried out, which only required the motor driver board. Subsequently, the EMG-driven control was developed; therefore, the EMG acquisition board was independently designed and incorporated.

C. EMG-DRIVEN CONTROL

The operation of the EMG-driven control can be summarized as (Fig. 3): the EMG signals of the target muscles of the healthy forearm are recorded by the custom-made EMG acquisition system using surface electrodes. The EMG acquisition system transmits the discrete bio-signals to the LAUNCHXL-F28069M via SPI communication, which is also required other control signals, e.g., data ready (DR) and reset (RST) signals. The DR signal indicates whether a new conversion result is ready to be read, and it is used as an interrupt input of the microcontroller to acquire the raw EMG data immediately after analog-to-digital conversion. The CLA core is used for the calculation of the rectified EMG signals (a time-critical task), thereby freeing up the main CPU. The normalized values of the processed EMG signals are sent to the C28x core, which determines the desired position of the actuators according to the EMG-driven control algorithm and applies the appropriate PWM signals to each actuator.

The final solution is a device capable of recording EMG signals in real-time, while the high performance of the TMS320F28069M MCU is used for on-board processing. The overall system (EMG data acquisition system and LAUNCHXL-F28069M) provides an embedded solution for real-time EMG-based hand gesture recognition for controlling the exoskeleton.

III. EMG-DRIVEN CONTROLLER FOR HAND-ASSISTED BILATERAL HAND REHABILITATION

The EMG-driven mode controls the motion of the exoskeleton based on the EMG processed signals collected from the

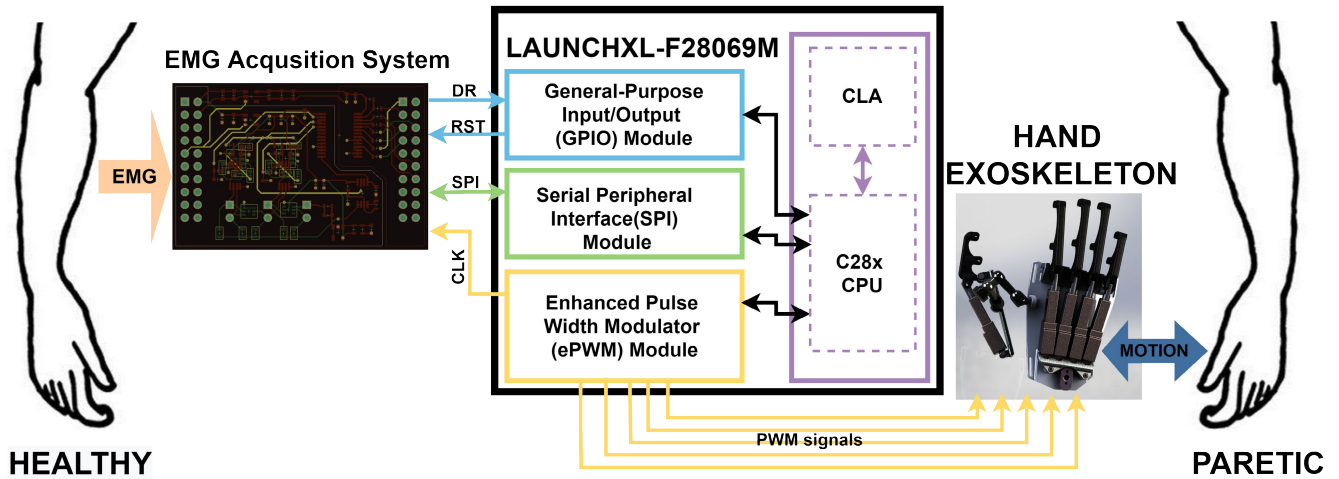


FIGURE 3. Simplified block diagram of the EMG-driven control of RobHand for assisted bilateral therapy.

muscles of the forearm which are responsible for the hand opening and closing motion, that is, the patient’s intention.

A. EMG SIGNAL CAPTURE AND NORMALIZATION

The detection of the hand motion or intention of motion, particularly hand opening and closing, is necessary to control the exoskeleton. This detection is achieved by recording the sEMG signals of the muscles responsible for the flexion and extension of the fingers of the hand. The selection of the muscles for sensor placement is a difficult issue to address because humans have up to 40 muscles that influence the movement of both the hand and wrist, and some of these muscles are split into different muscle compartments [25]. Some of the muscles involved in hand opening and closing are as follows: abductor pollicis brevis (APB), abductor pollicis longus (APL), flexor digitorum superficialis (FDS) and extensor digitorum (ED).

These muscles are either located at the forearm or the palm. Due to space limitations caused by that the hand exoskeleton (when placed on the hand), only the muscles of the forearm are considered for measurement in the case of EMG-driven unilateral therapy. Consequently, the EMG signals from the extensor digitorum (ED) and the flexor digitorum superficialis (FDS) muscles are recorded, which are responsible for the hand opening and closing. Two pairs of surface electrodes (Lessa-AB Medica Group, with a contact area of 30 × 30 mm) are placed on the skin surface of the belly of the target muscles with a center distance of 3 cm (recommended by SENIAM [78]), while the reference electrode is attached to the skin surface of the olecranon.

EMG signals must be normalized to compare EMG activity between muscles [79]. EMG normalization is important because of the interference that affects the signals, such as power line noise, skin perspiration, sensor contact impedance, which causes high signal variability, and the crosstalk interference from active muscles. Furthermore, small differences of the placement of the electrodes between

sessions compromise the repeatability of the EMG signals [80]. EMG processing maps the raw EMG signal into a normalized signal in the range of [0, 1], where a value of 1 stands for the maximal voluntary contraction (MVC) of the muscle. Normalization implies the previous rectification of the raw EMG signal.

The raw signals are recorded by a custom-made EMG acquisition system using surface electrodes with a sampling frequency of 200 Hz and are transmitted to the TMS320F28069M MCU to carry out the filtering, rectification and normalization of the signals (Fig. 4).

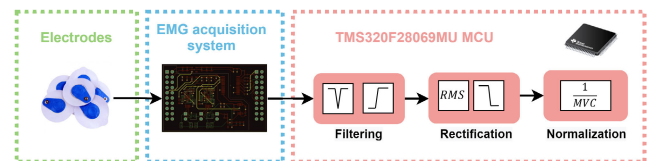


FIGURE 4. sEMG signal normalization: from the acquisition of the signals to their normalization.

First, the signals are filtered with a notch filter (center frequency of 50 Hz and Q-factor of 20) and a high-pass FIR filter (stopband frequency of 0.01 Hz, passband frequency of 10 Hz, minimum stopband attenuation at 80 dB and maximum passband ripple of 0.1 dB) to remove the offset and eliminate electromagnetic interference. The filtered signals are rectified by calculating the root mean square (RMS) with a 10 point window and then applied to a low-pass FIR filter (passband edge frequency of 1 Hz, stopband edge frequency of 2 Hz, maximum passband ripple of 4 dB and minimum stopband attenuation of 10 dB) to produce a smother representation of the envelope signal. The resulting rectified signal has a period of 20 ms and is normalized with respect to the previously measured MVC values of the patient. Fig. 6 (top and middle) shows the raw EMG signals and their corresponding normalized signals from FDS and ED muscles.

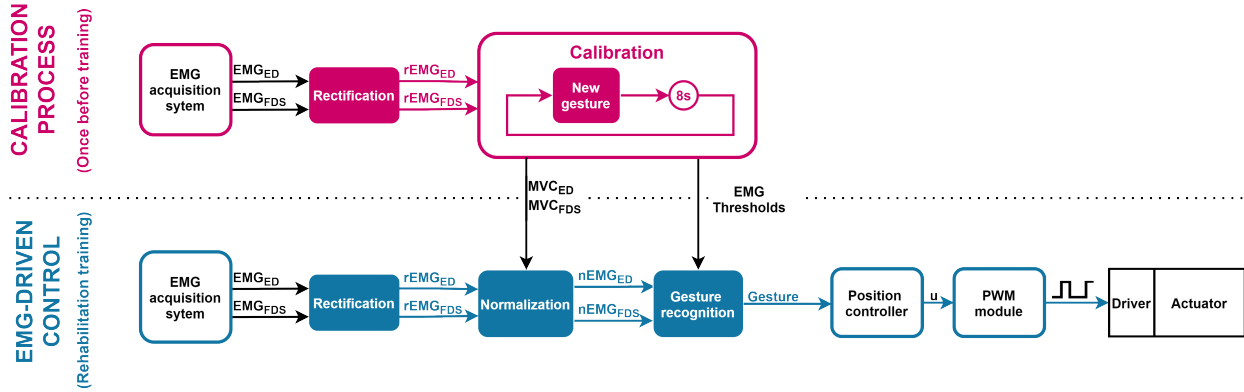


FIGURE 5. Control loop for the calibration process and the threshold EMG-driven control of RobHand.

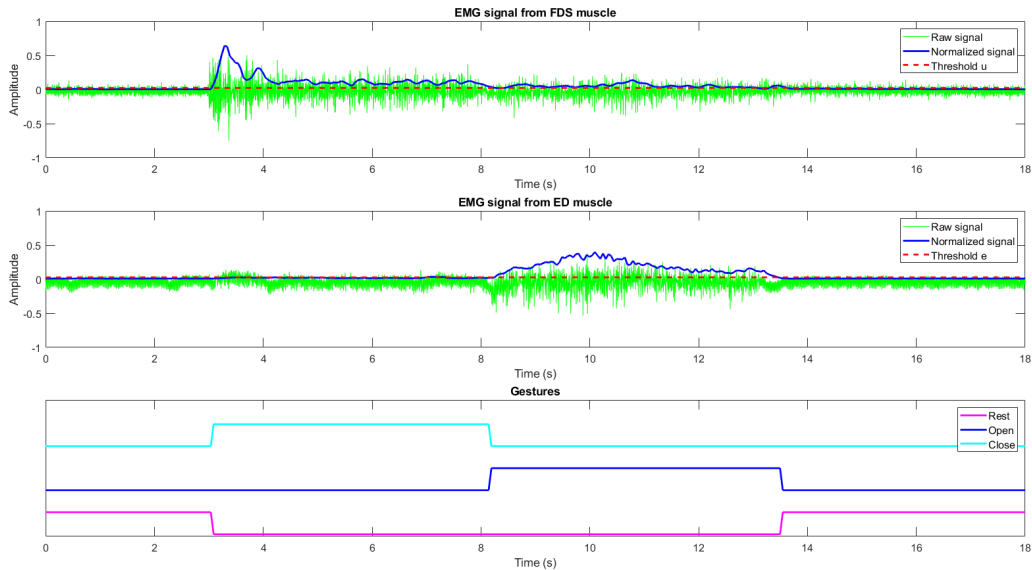


FIGURE 6. EMG signal treatment of the bio-controller for the proposed threshold EMG-driven control: raw EMG signals of ED and FDS muscles, normalized EMG signals, thresholds and determined gestures.

B. CALIBRATION PROCESS

For each subject, a calibration procedure should be performed once before starting a rehabilitation session to calculate the necessary thresholds for the EMG-driven control and to determine the MVC values, which are necessary for normalizing the EMG signals.

Subjects are asked to perform a trial that consists of relaxing the hand and performing maximum finger flexion and extension for 8 s, while the action and muscle activity are displayed to the subject on the computer screen (Fig. 5).

The MVC corresponds to the maximum voluntary contraction and the MVC values of each muscle (MVC_{ED} and MVC_{FDS}) are computed as the maximum value of their corresponding rectified EMG signal ($rEMG$) during the calibration.

$$MVC_{FDS/ED} = \max(rEMG_{FDS/ED}) \quad (1)$$

Two EMG thresholds values (μ and ε) are determined during the calibration session, which are the maximum limit values corresponding to muscular deactivation (in other words, they are the onset of the muscle activation) plus a constant of 0.1. The flexor threshold (μ) corresponds to the FDS muscle and the extensor threshold (ε) corresponds to the ED muscle. The top and middle graphs of Fig. 6 show the thresholds.

$$\varepsilon = \frac{\min(rEMG_{ED})}{MVC_{ED}} + 0.1 \quad (2)$$

$$\mu = \frac{\min(rEMG_{FDS})}{MVC_{FDS}} + 0.1 \quad (3)$$

C. THRESHOLD EMG-DRIVEN CONTROL

The threshold EMG-driven control can perform bilateral training by recognizing the actual gesture of the healthy hand and replicating that gesture on the hand exoskeleton placed

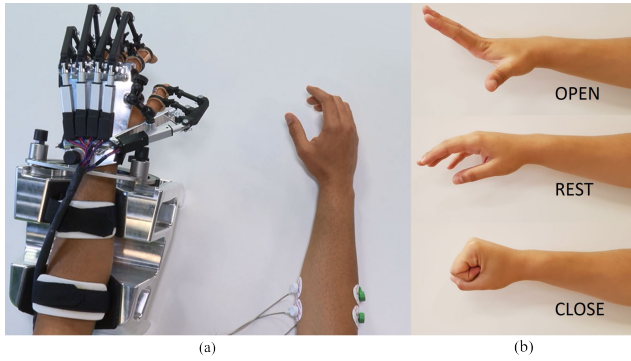


FIGURE 7. Bilateral assisted training with the RobHand exoskeleton, which replicates three predefined hand gestures.

on the paretic hand (Fig. 7a). For this goal, three possible gestures of the exoskeleton are defined: “rest hand”, “open hand” and “closed hand” (Fig. 7b).

The operation of the threshold EMG-driven control is as follows: the microcontroller rectifies and normalizes the sEMG signals captured from two muscles on the healthy forearm (ED and FDS muscles) to determine the actual gesture of the healthy hand to provide the proper pulse width modulation (PWM) signal to the exoskeleton actuators for achieving the target gesture of the paretic hand (rest, open or closed hand) (Fig. 5).

The gesture recognition module updates the gesture each 20 ms (normalized EMG signal update period) according to the following algebraic expressions:

$$REST = \bar{A} \cdot \bar{B} \quad (4)$$

$$OPEN = A \cdot (\bar{B} + C) \quad (5)$$

$$CLOSE = B \cdot (\bar{A} + \bar{C}) \quad (6)$$

For any combination of inputs, only one of the outputs (REST, OPEN or CLOSE) is true:

$$A \rightarrow nEMG_{ED} > \varepsilon \quad (7)$$

$$B \rightarrow nEMG_{FDS} > \mu \quad (8)$$

$$C \rightarrow nEMG_{ED} > nEMG_{FDS} \quad (9)$$

The determination of the gesture only depends on the values of the normalized EMG signals (nEMG) and the two EMG thresholds values (μ and ε), which are set based on the initial calibration of each subject according to its residual muscle activity.

The closed hand gesture is recognized when the normalized signal from the FDS muscle crosses over the flexor threshold μ while the normalized signal from FDS muscle is larger than the normalized signal from ED muscle if it exceeds the extensor threshold ε . Consequently, the actuators reach maximum stroke extension and the hand exoskeleton is completely closed. Similarly, the open hand gesture is recognized when the ED muscle signal crosses over the extensor threshold ε , while the normalized signal of the ED muscle is larger than the FDS muscle normalized signal if it exceeds

the flexor threshold μ . Consequently, the actuators reach their minimum stroke extension and the hand exoskeleton is completely opened. The rest gesture is recognized when both EMG normalized signals are lower than their respective threshold, and the hand exoskeleton presents the rest gesture (Fig. 6).

A person performing assisted bilateral rehabilitation using the proposed threshold EMG-driven control system with the RobHand exoskeleton can be found in the attached multimedia movie clip in MP4 format.

IV. CONTROLLER AND SYSTEM DELAYS: EXPERIMENTAL STUDY

A reliable human-robot interaction (HRI) in rehabilitation robotics is critical for improving the user acceptance and therefore achieving good rehabilitation outcomes. Proper rehabilitation implies a good natural HRI; therefore, the controller must have a high accuracy and small latency time since excessive latency can lead to frustration, boredom or negative feelings in the patient, thereby generating poor results in rehabilitation, which can lead to unfavorable situation, including the rejection of rehabilitation treatment.

Therefore, we have performed several tests to evaluate the performance of the robotic rehabilitation platform overall, including the low-cost custom-made EMG acquisition system, the onboard threshold EMG-driven control system (including the bio-controller and the position controller) and the electromechanical behavior of the exoskeleton. We intend to validate the proposed application of an embedded implementation of EMG signal processing in the context of the bilateral control of RobHand rehabilitation platform and show that it provides limited latency and high accuracy, adequate proprioceptive perception by the user is adequate, and a satisfactory rehabilitation experience.

A. EXPERIMENTAL DESIGN: SUBJECTS AND TRIALS

The experiments were performed with ten healthy subjects (3 females and 7 males; age range: 22-26 years) with no neurological or orthopedic impairment who volunteered for this study and provided written informed consent.

The experiments (Fig. 8) required the following resources: (a) 5DT Data Glove (5DT Technologies) to measure the actual position of the dominant hand (which would correspond to the non-paretic hand of the patient); (b) the RobHand exoskeleton attached to the non-dominant hand (which would correspond to the paretic hand of the patient) that records the EMG signals of the target muscles of the dominant hand.

The subjects were asked to perform a calibration and then ten one-minute tests, with a 5-minute rest between tests to avoid muscle fatigue. Each test consisted of performing hand gestures (rest, open and close) with the dominant hand while simultaneously recording its movement using the 5DT Data Glove and collecting the data from the RobHand system (EMG signals of the dominant forearm and both control signal and position of the exoskeleton placed on the non-dominant hand). The sequence of gestures to be performed

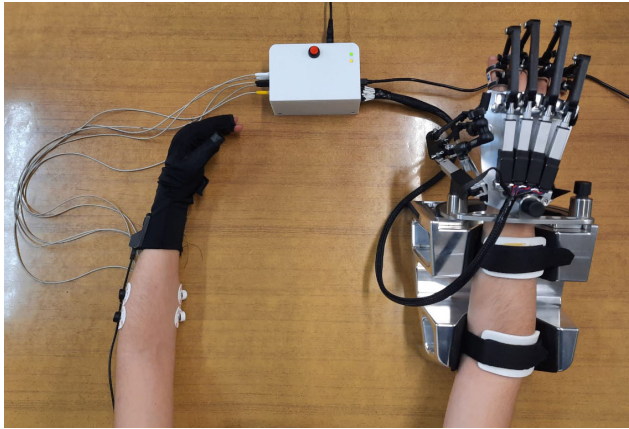


FIGURE 8. Experimental setup. The subject (left-handed) is wearing the 5DT data glove on her dominant hand and the exoskeleton on her non-dominant hand, while recording the EMG signals of the target muscles of the forearm of the dominant hand.

in each test was randomly generated, and each gesture had a duration of 5 s. The gesture that the user must perform at each instant was shown on a computer screen.

B. PERFORMANCE METRICS

There is no clear consensus in the academic literature about the concepts of “delay” and “lag”. For this reason, we will first and foremost provide definitions of both. Lag is considered the delay experienced by the user when using a system (subjective and not measurable in time), while delay is considered the time between an input and a certain response from the system (objective and measurable in time, such as the computational delay). Large delay times can exert negative consequences (e.g., decreasing the accuracy of task completion, reducing perceptual sensitivity, increasing the task error rate, etc.) and can negatively influence the emotional state, arousal, and satisfaction of the user [81]. For this reason, it is important to identify the time delays of the system that are relevant to the human-robot interaction. The following time metrics are used:

1) MOTION-SELECTION TIME (MST)

Time needed by the controller to accurately determine the hand gesture (open, close, rest). Motion-selection time is calculated as the time interval from the onset of the hand gesture change movement (detected by the glove) to the instant the controller accurately predicts the following gesture.

2) MOTION-ONSET TIME (MOT)

Motion-onset time is calculated as the time interval from the onset of the hand gesture change movement (detected by the glove) to the instant the exoskeleton starts the movement (detected by the position feedback of the actuators).

3) MOTION-COMPLETION TIME (MCT)

Motion-completion time is calculated as the time interval from the onset of the hand gesture change movement

(detected by the glove) to the instant the exoskeleton correctly reaches the next hand gesture (detected by the position feedback of the actuators).

4) MOTION-COMPLETION RATE

The motion-completion rate is the percentage of successfully motions. A motion is considered successful when it is performed within a time limit (established at 5 s) [82]. The time limit is based on clinical experience; thus, the motion is not too slow, which may annoy and demotivate the user with regard to the rehabilitation therapy.

In Fig. 9, a timing diagram is shown in which the aforementioned time values (MST, MOT, and MCT) are shown to facilitate a better understanding. These time values are characterized by events that indicate the start or end time of them. These events are the motion onset time of the dominant hand of the subject (MO_{HAND}), the motion onset time of the exoskeleton (MO_{EXO}), the motion end time of the exoskeleton (ME_{EXO}) and the time in which the controller accurately detects the hand gesture (AGD_{CTRL}). Other time values are shown in Fig. 9: electromechanically delay (ED), computational time (CPT) and latency of the controller ($Latency_{CTRL}$).

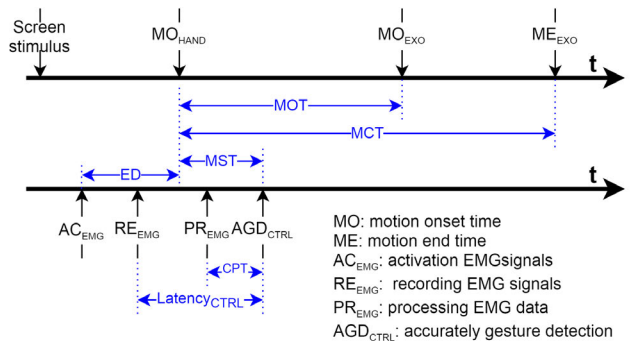


FIGURE 9. Timing diagram showing the following time parameters: MST, MOT, MCT, ED, CPT and $Latency_{CTRL}$.

Furthermore, the accuracy, precision and recall are calculated to evaluate the performance of the EMG-threshold gesture recognition module in isolation. To determine these metrics, the actual gestures adopted by the dominant hand are determined from the data provided by the 5DT Data Glove.

5) ACCURACY

The accuracy is the ratio of correctly predicted gestures over the total number of gestures.

$$Acc = \frac{TP + TN}{TP + FP + FN + TN} \quad (10)$$

6) PRECISION OR POSITIVE PREDICTIVE VALUE (PPV)

This value is the ratio of the true positives over the sum of true positives and false positives.

$$PPV = \frac{TP}{TP + FP} \quad (11)$$

7) RECALL OR TRUE POSITIVE RATE (TPR)

This rate is the ratio of true positives over the sum of true positives and false negatives.

$$TPR = \frac{TP}{TP + FN} \tag{12}$$

where TP (true positives) is the number of times the bio-controller detects a gesture when the gesture is present; TN (true negatives) is the number of times the bio-controller does not detects the gesture when the gesture is absent; FP (false positives) is the number of times the bio-controller detects the gesture when the gesture is absent; and FN (false negatives) is the number of times the bio-controller does not detect the gesture when the gesture is present.

C. EXPERIMENTAL RESULTS

To our knowledge, no objective work has been performed to determine the impact of the controller latency and its optimal value for rehabilitation robots, and very few results have been published for prosthetics [83]. For prostheses, the optimal latency ($Latency_{CTRL}$ in Fig. 9), which is the time taken by the control system to perform processing, from the signal recording to correct classification has been established at between 100 and 150 ms, with the maximum tolerable latency limit at approximately 300 ms [84], [85]. On the other hand, 5 s is considered the maximum limit of the MCT, which prevents the user from getting frustrated because of the slow response of the prosthesis device [82]. Although the optimal latency depends on the application [86], it could be considered that the established times for prostheses may be adequate for robotic hand rehabilitation systems; however, the latency in robotic rehabilitation applications is not as critical as that for prosthetics. Moreover, the optimal latency does not provide actual information about the lag that the user would experience when using the system and only provides partial information about the lag.

Therefore, a complete study of time delays of the RobHand system has been carried out, and the motion-selection time, motion-onset time and motion completion time (some used in [82]) have been calculated. In Fig. 10, the temporal metrics are reported. The average of the MST and the MOT are

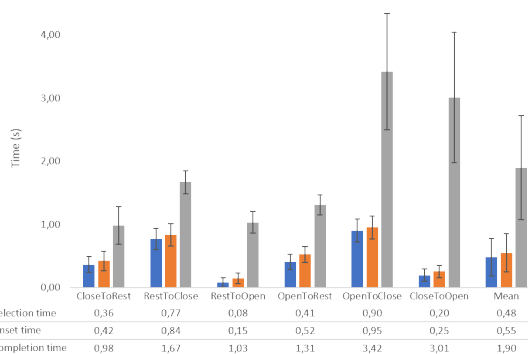


FIGURE 10. Results of the motion-selection, motion-onset and motion-completion times obtained from the experimental trials.

0.48 ± 0.59 s and 0.55 ± 0.60 s, respectively. The average of the MCT is 1.90 ± 1.65 s, and it varies from 0.98 s (close to rest movement) to 3.42 s (open to close movement). The MCT values, which are dependent on the actuators speed, are not excessively short to ensure the subject’s safety, and all of them are below the established time limit (5 s) for all performed tests. Consequently, the motion-completion rate is 100% to guarantee the performance reliability of the system.

A confusion matrix is calculated from the data obtained from the actual hand gestures (determined by the 5DT Data Glove) and the predicted gestures (determined by the gesture recognition module of the bio-controller). Fig. 11 shows the results obtained by removing the gesture transition period that starts when a transient gesture is detected by the glove with an average duration of 0.9 s (corresponding to the maximum MST obtained from the experimental trial), which eliminates detected gestures that would be considered erroneous (but are not) because of the time latency induced by the bio-controller when detecting the gesture from the EMG signals.

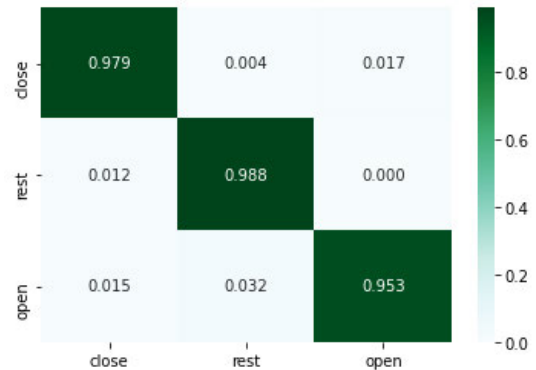


FIGURE 11. Confusion matrix obtained without considering the data points of the gesture transitions.

V. DISCUSSION

A comparison of the calculated temporal metrics with the values of other similar works would provide interesting data. However, carrying out a comparison of the latency of our system with other previous works of robotic hand rehabilitation platforms is a difficult issue because of the lack of published data.

For this comparison, a systematic review has been conducted according to PRISMA (Reporting Items for Systematic Reviews and Meta-Analyses), and the following question was established during the systematic review process: “What is the latency time of EMG-driven robotic platforms for hand rehabilitation?” A literature search was carried out in March 2021 in IEEE Xplore, Web of Science, and PubMed databases, and it included all articles published to date. The following keywords were used in the database search according to the abovementioned question: (1) hand, (2) *emg* or myo* or electromyograph*, (3) robot or exoskeleton, (4) rehabilitation or training. In addition, the (1), (2), (3) keywords must be included in the article title while the (4) keyword must appear in the article title or abstract. Based on the above,

the following Boolean expressions were created and inserted in the search bar of each database:

–IEEE Xplore: (((“Document Title”:HAND) AND (“Document Title”: “*emg*” OR “myo*” OR “electromyograph*”) AND (“Document Title”: “robot*” OR “exoskeleton”) AND (“Document Title”: “rehabilitation” OR “training”) OR (“Abstract”: “rehabilitation” OR “training”))))

–Web of Science: ((TI = ((hand) AND (*emg* OR myo* OR electromyograph*)) AND (robot* OR exoskeleton))) AND ((AB = (rehabilitation OR training)) OR (TI = (rehabilitation OR training))))

–PubMed: (hand [Title]) AND (*emg* [Title] OR myo*[Title] OR electromyograph*[Title]) AND (exoskeleton [Title] OR robot*[Title]) AND (rehabilitation [Title/Abstract] OR training [Title/Abstract]))

The inclusion/exclusion criteria were as follows: (1) the articles must be written in English, (2) the articles must be about EMG-driven robots, excluding multimodal controls, which use EMG in combination with data from other sensors; (3) the articles need to be specific for hand rehabilitation; and (4) the articles must use an actual rehabilitation robot, excluding those that use a virtual hand or a protheses.

Initially, 43 records were retrieved (9 from IEEE Xplore, 21 from Web of Science, and 13 from PubMed databases) with the previously established Boolean expressions and setting the search for articles only. Only 38 of the 43 found records were journals articles (9 from IEEE Xplore, 19 from Web of Science, and 10 from PubMed databases). After removing 13 duplicates (34.21%), the search was reduced to 25 articles. From these, 8 articles were excluded based on the title and abstract, which indicated that they were not focused in the topic. From the 17 remained articles, 8 articles were excluded because they did not meet the content criteria or were written about the same robotic platform (in this case, the most complete and recent article has been selected). Finally, only nine (collected in Table 1 and Table 2) met the inclusion/exclusion criteria and were considered for this systematic review, and only two ([69], [70]) included latency times. The selection procedure is summarized in Fig. 12.

The study in [69] is an exceptional case that provides a time analysis of an EMG-driven hand exoskeleton (commercially available under the brand name ‘Hand of Hope’), which can detect six different hand gestures. Five time parameters are provided in this study: “algorithm lag”, “total lag”, “motion period”, “waiting period” and “completion time”. The “algorithm lag” (CPT in Fig. 9) is defined as the time for data processing (38 ms) and the “total lag” as the time for data acquisition, processing and transmission (250 ms). They define the “motion period” (MP = ME_{EXO}-MO_{EXO}) as the time in which the exoskeleton executes commands, and it is determined by the mechanical design of the exoskeleton, which was 4-5 s. The “waiting period” (WP) is defined as the time in which the exoskeleton waits for commands, which indicates the time required by the subject to trigger the robot (3 s for healthy subjects). The “completion time” (CT) is defined as the time a subject uses to complete a motion, which

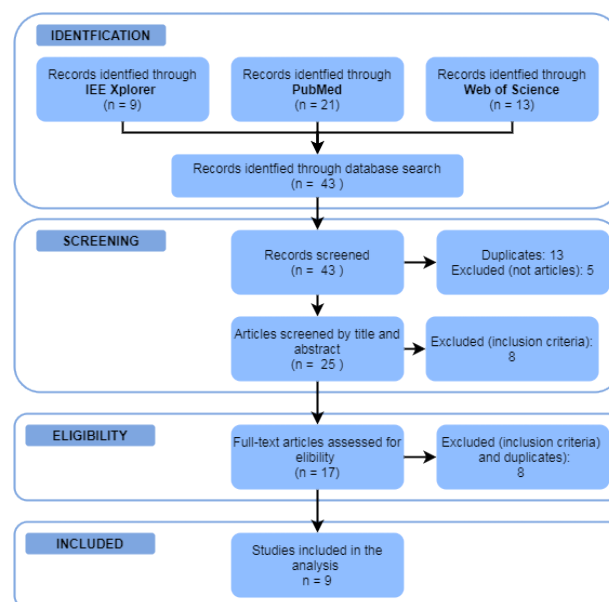


FIGURE 12. Bibliographic search using PRISMA flowchart.

begins when the exoskeleton completes a motion and ends when the exoskeleton completes the following motion (CT = MP + WP). These values are hardly comparable with the ones calculated in our work: only the MP can be compared, and their value is significantly larger than ours (varying from 0.6 for close to rest movement to 2.7 s for close to open movement). Furthermore, we consider that the time values do not provide clear information about the lag that the user would experience when using the robot. We think that the “algorithm lag” is irrelevant for the lag and the “total lag” does not consider how fast the exoskeleton processes the commands; therefore, when the actuators start moving, the “motion period” mainly depends on the speed of the actuators, the “waiting period” is not conclusive, and the “completion time” is not completed either since it explicitly depends on when the user decides to perform the hand movement.

In [70], the “control speed” is measured as the number of actions (rest, fist, wave in, wave out, fingers spread and double tap) correctly performed in one minute, which is 42.86 actions/min on average. Consequently, the mean “time per action” is 1.4 s. This value is comparable with the previously calculated MCT, which is significantly larger (MCT_{ROBHAND} = 1.90±1.65 s, ranging from 0.98 s for the close to rest movement to 3.42 s for the open to close movement). However, we think that our time values are adequate considering that the device is used for rehabilitation purposes and the patient’s safety must be ensured by applying an adequate speed of the actuators. On the other hand, we think that the “time per action” value alone does not provide enough information about the lag. For example, the computational time (CPT in Fig. 9) could be very large while the actuators could be very fast (small MP time), resulting in a low “time per action” (note that the speed of the actuators presents a greater contribution to the total time than the computational time).

TABLE 2. Published data on the accuracy and time information of EMG-driven hand rehabilitation robots.

Ref	Control type	Accuracy	Delay ⁽²⁾
[53]	Point-in-Polygon (PIP) (3 predefined gestures)	Accuracy: 0.944	-
[57]	EMG-driven (neural network to determine force)	Force error = 20.7 %	-
[68]	Threshold algorithm	-	-
[69]	Linear Bayes classifier (6 predefined gestures)	Accuracy ⁽¹⁾ : 98.1±4.9%	Yes
[70]	Classification algorithm (6 predefined gestures)	Accuracy: 86.38 %	Yes
[71]	EMG-based intent inference method	-	-
[72]	Neural network	-	-
[73]	Forest classifier (3 predefined gestures)	Accuracy: 77.9-85.2 %	-
[74]	Neural Network (4 predefined gestures)	Accuracy: 98.7±0.53	-

⁽¹⁾ Accuracy for neurologically intact subjects. ⁽²⁾ Whether delay analysis of the system is carried out.

Broadening the bibliographic search to consider embedded systems for EMG gesture recognition, which could be integrated in hand rehabilitation robots (even though the robot is not specified), we found that some authors specify the computational time (CPT). However, they only specify the computational time of the classification algorithm (without considering the EMG acquisition and data preprocessing), which is within 0.58-2.8 ms [47], [64], [66]; therefore, comparisons are not possible.

More information about control latency is available in the bibliography if hand prostheses based on EMG are also considered. For instance, in [87], the “time from the intended motion of the user until execution of the motion” is 600 ms. In [84], the “correct recognition of a transition to a different gesture” is 100-200 ms. In [88], the time “guarantees that the user can control a directed myoelectric hand function within 250 ms from the instant when the user’s intention is given”, but it does not specify whether the control is correct. However, no reliable comparison can be made with these aforementioned systems because we do not consider the provided values to be accurately defined and the provided time period (e.g., the onset and the end time of the measurement) is uncertain.

Regarding the accuracy of the bio-controller, the results of the confusion matrix (Fig. 11) are encouraging: the overall accuracy of the gesture recognition module is 0.97. Moreover, when analyzing the data in greater depth, misclassifications of the time during the gesture are very small (≤ 0.06 s); therefore, in 98.4% of cases, the error is not perceived in the exoskeleton (the actuators do not move in the opposite direction to the target direction or do not move if they are already in the target position). It is critical that the misclassifications usually last a short time because if they last for a period long enough to be perceived, an additional stress may be experienced by the user, which may cause them frustration and could even imply a harmful situation. Finally, the accuracy results are within the range of other control systems proposed in the literature and vary from 77.9% to 98.7 % (see Table 2).

The novelty of the presented solution is that it provides embedded real-time control using a low-cost EMG acquisition system to perform bio-cooperative rehabilitation therapies with a hand exoskeleton. The combination of

these two features has not been provided in previous related works (see Table 1). The EMG acquisition device has been designed to be as simple as possible and include the minimum components while ensuring reliability, which will reduce the price as much as possible. In this way, the designed 2-channel EMG acquisition device costs approximately 30€ for low-scale production. The price is small compared to that in previous works, which developed EMG acquisition systems at costs of \$199, \$500 and even more, and the cost is only similar to the system used in [53], which is \$37.95. The intrinsic advantage of performing real-time control within the TMS320F28069M embedded solution is that the latency of the system is reduced while achieving good gesture recognition accuracy.

VI. CONCLUSION

In this paper, a low-cost compact system that provides an embedded solution for real-time exoskeleton EMG-driven control has been presented. The designed EMG data acquisition ASIC can record EMG signals, and an onboard real-time EMG signal processing and control system is included, which reduces the cost of the whole system while providing good detection of the user’s intention and replication of the identified movement in the hand exoskeleton.

Many sEMG-based pattern recognition methods have been proposed in the literature for detecting hand gestures, and they have provided excellent results; however, they are not applicable in real cases because numerous DoFs are required for the robot and they have high computational costs and thus cannot be implemented in real-time embedded systems. For this reason, the bio-cooperative controller of RobHand incorporates an EMG threshold gesture recognition module to drive the five-active-DOF hand exoskeleton. A non-pattern recognition method has been implemented because its simplicity allows it to be implemented in a real-time embedded system without compromising the reliability.

A preliminary study has been conducted to validate its performance based on the accuracy and responsiveness (including a comprehensive study of latency times). Our study, which was carried out with healthy subjects, can be extrapolated to people suffering from stroke who only have one affected hand because the control is performed bilaterally: the sEMG signals of the non-paretic forearm of the subject determine

the behavior of the exoskeleton and the paretic member does not affect the system performance.

The EMG threshold control, which allows for the recognition of three predefined positions (open, relax and close), has an accuracy of a 97% and a motion-completion rate of 100%, thus indicating high system reliability. The responsiveness of the system has been studied by determining three temporal metrics (0.48 ± 0.59 s for motion-selection time, 0.55 ± 0.60 s for the motion-onset time and 1.90 ± 1.65 s for motion-completion time). However, these metrics are difficult to compare with previously works because available data are limited. When designing and developing the rehabilitation system, we have tried to minimize the latency time as much as possible by 1) obtaining the EMG signals for software processing immediately after ADC conversion at 200 Hz via SPI communication; 2) exploiting the high performance of the TMS320F28069M MCU and implementing EMG processing and control in the CLA core; 3) designing an EMG processing algorithm (selection of the filters, method of rectification and time window) for use with the custom-made EMG board and the CLA core of the TMS320F28069M MCU, which can reduce the latency while ensuring the quality of the normalized signal; and 4) generating the control signal of the actuators by the embedded system and computing the EMG normalization to prevent transmission latency time (in previous works, the EMG processing is performed in the PC, which requires the data to be transmitted from the PC to the microcontroller that controls the actuators).

Previously works on EMG-driven rehabilitation systems have not given high priority to the responsiveness of the system (latency times are not provided) and only focused on evaluating the accuracy of the hand gesture classifier. Other works on EMG-driven hand prosthetics provided more information about the responsiveness of the system, although the measured latency was not clear and should be more precisely defined. For these reasons, we believe that efforts should be made to establish the most important latency times, which should be considered when developing rehabilitation robotics, and to define them both accurately and generically to provide a standard for homogenizing all the work of this area of knowledge.

In summary, the proposed EMG-driven control in combination with the low-cost embedded real-time EMG solution is reliable for performing bilateral assisted rehabilitation therapy and the RobHand exoskeleton moves the impaired hand by replicating the movement of the healthy hand, and it presents tolerable response times and accuracy.

REFERENCES

- [1] World Health Organization. (2018). *The Top 10 Causes of Death*. [Online]. Available: <https://www.who.int/news-room/fact-sheets/detail/the-top-10-causes-of-death>
- [2] W. Johnson, O. Onuma, M. Owolabi, and S. Sachdev, "Stroke: A global response is needed," *Bull. World Health Org.*, vol. 94, no. 9, pp. 634A–635A, 2016.
- [3] M. E. Parker and M. Snyder-Shall, "Recovery of upper extremity function in stroke patients," *Neurol. Rep.*, vol. 19, no. 1, pp. 46–47, 1995.
- [4] T. B. Wyller, J. Holmen, P. Laake, and K. Laake, "Correlates of subjective well-being in stroke patients," *Stroke*, vol. 29, no. 2, pp. 363–367, Feb. 1998.
- [5] E. J. Jonkman, A. W. Weerd, and N. L. H. Vrijens, "Quality of life after a first ischemic stroke," *Acta Neurologica Scandinavica*, vol. 98, no. 3, pp. 169–175, Sep. 1998.
- [6] S. S. Rathore, A. R. Hinn, L. S. Cooper, H. A. Tyroler, and W. D. Rosamond, "Characterization of incident stroke signs and symptoms: Findings from the atherosclerosis risk in communities study," *Stroke*, vol. 33, no. 11, pp. 2718–2721, Nov. 2002.
- [7] H. C. Fischer, K. Stubblefield, T. Kline, X. Luo, R. V. Kenyon, and D. G. Kamper, "Hand rehabilitation following stroke: A pilot study of assisted finger extension training in a virtual environment," *Top. Stroke Rehabil.*, vol. 14, no. 1, pp. 1–12, 2007.
- [8] D. G. Kamper, R. L. Harvey, S. Suresh, and W. Z. Rymer, "Relative contributions of neural mechanisms versus muscle mechanics in promoting finger extension deficits following stroke," (in English), *Muscle Nerve*, vol. 28, no. 3, pp. 309–318, Sep. 2003.
- [9] J. G. Colebatch and S. C. Gandevia, "The distribution of muscular weakness in upper motor neuron lesions affecting the arm," *Brain*, vol. 112, no. 3, pp. 749–763, 1989.
- [10] L. Ada, "Stroke patients have selective muscle weakness in shortened range," *Brain*, vol. 126, no. 3, pp. 724–731, Mar. 2003.
- [11] A. Sterr and S. Freyvogel, "Motor-improvement following intensive training in low-functioning chronic hemiparesis," *Neurology*, vol. 61, no. 6, pp. 842–844, Sep. 2003.
- [12] E. M. Frick and J. L. Alberts, "Combined use of repetitive task practice and an assistive robotic device in a patient with subacute stroke," *Phys. Therapy*, vol. 86, no. 10, pp. 1378–1386, Oct. 2006.
- [13] P. Polygerinos, Z. Wang, K. C. Galloway, R. J. Wood, and C. J. Walsh, "Soft robotic glove for combined assistance and at-home rehabilitation," *Robot. Auto. Syst.*, vol. 73, pp. 135–143, Nov. 2015.
- [14] E. Carmeli, S. Peleg, G. Bartur, E. Elbo, and J.-J. Vatine, "HandTutorTM enhanced hand rehabilitation after stroke—a pilot study," *Physiotherapy Res. Int.*, vol. 16, no. 4, pp. 191–200, Dec. 2011.
- [15] S. Ueki, Y. Nishimoto, M. Abe, H. Kawasaki, S. Ito, Y. Ishigure, J. Mizumoto, and T. Ojika, "Development of virtual reality exercise of hand motion assist robot for rehabilitation therapy by patient self-motion control," in *Proc. 30th Annu. Int. Conf. IEEE Eng. Med. Biol. Soc.*, Aug. 2008, pp. 4282–4285.
- [16] N. G. Kutner, R. Zhang, A. J. Butler, S. L. Wolf, and J. L. Alberts, "Quality-of-life change associated with robotic-assisted therapy to improve hand motor function in patients with subacute stroke: A randomized clinical trial," *Phys. Therapy*, vol. 90, no. 4, pp. 493–504, Apr. 2010.
- [17] S. L. Wolf, C. J. Winstein, J. P. Miller, E. Taub, G. Uswatte, D. Morris, C. Giuliani, K. E. Light, and D. Nichols-Larsen, "Effect of constraint-induced movement therapy on upper extremity function 3 to 9 months after stroke," *JAMA*, vol. 296, no. 17, p. 2095, Nov. 2006.
- [18] G. Kwakkel, B. J. Kollen, and H. I. Krebs, "Effects of robot-assisted therapy on upper limb recovery after stroke: A systematic review," *Neurorehabil. Neural Repair*, vol. 22, no. 2, pp. 111–121, Jan. 2008.
- [19] J. S. Rietman, G. Prange, A. Kottink, G. Ribbers, and J. Buurke, "The effect of an arm supporting training device in sub-acute stroke patients: Randomized clinical trial," *Arch. Phys. Med. Rehabil.*, vol. 95, no. 10, p. e8, Oct. 2014.
- [20] Z. Yue, X. Zhang, and J. Wang, "Hand rehabilitation robotics on poststroke motor recovery," *Behavioural Neurol.*, vol. 2017, pp. 1–20, Nov. 2017.
- [21] B. D. Schmit, J. P. A. Dewald, and W. Z. Rymer, "Stretch reflex adaptation in elbow flexors during repeated passive movements in unilateral brain-injured patients," *Arch. Phys. Med. Rehabil.*, vol. 81, no. 3, pp. 269–278, Mar. 2000.
- [22] B. Volpe, H. Krebs, N. Hogan, L. Edelstein, C. Diels, and M. Aisen, "A novel approach to stroke rehabilitation: Robot-aided sensorimotor stimulation," *Neurology*, vol. 54, no. 10, pp. 1938–1944, 2000.
- [23] R. K. Tong, M. F. Ng, and L. S. Li, "Effectiveness of gait training using an electromechanical gait trainer, with and without functional electric stimulation, in subacute stroke: A randomized controlled trial," *Arch. Phys. Med. Rehabil.*, vol. 87, no. 10, pp. 1298–1304, Oct. 2006.
- [24] C. Fleischer, A. Wege, K. Kondak, and G. Hommel, "Application of EMG signals for controlling exoskeleton robots," *Biomedizinische Technik/Biomed. Eng.*, vol. 51, nos. 5–6, pp. 314–319, Dec. 2006.
- [25] A. Wege and A. Zimmermann, "Electromyography sensor based control for a hand exoskeleton," in *Proc. IEEE Int. Conf. Robot. Biomimetics (ROBIO)*, Dec. 2007, pp. 1470–1475.

- [26] P. Heo, G. M. Gu, S. Lee, K. Rhee, and J. Kim, "Current hand exoskeleton technologies for rehabilitation and assistive engineering," *Int. J. Precis. Eng. Manuf.*, vol. 13, no. 5, pp. 807–824, May 2012.
- [27] Y. Li, Q. Zhang, N. Zeng, J. Chen, and Q. Zhang, "Discrete hand motion intention decoding based on transient myoelectric signals," *IEEE Access*, vol. 7, pp. 81630–81639, 2019.
- [28] L. Zhang, G. Liu, B. Han, Z. Wang, and T. Zhang, "SEMG based human motion intention recognition," *J. Robot.*, vol. 2019, pp. 1–12, Aug. 2019.
- [29] L. Lucas, M. DiCicco, and Y. Matsuoka, "An EMG-controlled hand exoskeleton for natural pinching," *J. Robot. Mechatronics*, vol. 16, no. 5, pp. 482–488, Oct. 2004.
- [30] M. Serpelloni, M. Tiboni, M. Lancini, S. Pasinetti, A. Vertuan, and M. Gobbo, "Preliminary study of a robotic rehabilitation system driven by EMG for hand mirroring," in *Proc. IEEE Int. Symp. Med. Meas. Appl. (MeMeA)*, May 2016, pp. 1–6.
- [31] M. Chen, S. K. Ho, H. F. Zhou, P. M. K. Pang, X. L. Hu, D. T. W. Ng, and K. Y. Tong, "Interactive rehabilitation robot for hand function training," in *Proc. IEEE Int. Conf. Rehabil. Robot.*, Jun. 2009, pp. 777–780.
- [32] P. Polygerinos, K. C. Galloway, S. Sanan, M. Herman, and C. J. Walsh, "EMG controlled soft robotic glove for assistance during activities of daily living," in *Proc. IEEE Int. Conf. Rehabil. Robot. (ICORR)*, Aug. 2015, pp. 55–60.
- [33] M. Gandolla, P. Milano, S. Ferrante, and P. Milano, "EMG-controlled robotic hand rehabilitation device for domestic training," in *Proc. 15th Mediterr. Conf. Med. Biol. Eng. Comput.*, vol. 57, 2016, pp. 644–648.
- [34] K. Kiguchi, T. Tanaka, and T. Fukuda, "Neuro-fuzzy control of a robotic exoskeleton with EMG signals," *IEEE Trans. Fuzzy Syst.*, vol. 12, no. 4, pp. 481–490, Aug. 2004.
- [35] K. Kiguchi, M. H. Rahman, and M. Sasaki, "Neuro-fuzzy based motion control of a robotic exoskeleton: Considering end-effector force vectors," in *Proc. IEEE Int. Conf. Robot. Autom. (ICRA)*, May 2006, pp. 3146–3151.
- [36] M. H. Rahman, K. Kiguchi, M. M. Rahman, and M. Sasaki, "Robotic exoskeleton for rehabilitation and motion assist," in *Proc. Int. Conf. Ind. Inf. Syst.*, Aug. 2006, pp. 8–11.
- [37] M. R. Ahsan, M. I. Ibrahimy, and O. O. Khalifa, "Electromyography (EMG) signal based hand gesture recognition using artificial neural network (ANN)," in *Proc. 4th Int. Conf. Mechatronics (ICOM)*, May 2011, pp. 1–6.
- [38] C. Choi and J. Kim, "A real-time EMG-based assistive computer interface for the upper limb disabled," in *Proc. IEEE 10th Int. Conf. Rehabil. Robot.*, Jun. 2007, pp. 459–462.
- [39] Y. Hu, H. Su, L. Zhang, S. Miao, G. Chen, and A. Knoll, "Nonlinear model predictive control for mobile robot using varying-parameter convergent differential neural network," *Robotics*, vol. 8, no. 64, pp. 2–21, 2019.
- [40] Y. Hu, J. Li, Y. Chen, Q. Wang, C. Chi, H. Zhang, Q. Gao, Y. Lan, Z. Li, Z. Mu, Z. Sun, and A. Knoll, "Design and control of a highly redundant rigid-flexible coupling robot to assist the COVID-19 oropharyngeal-swab sampling," *IEEE Robot. Autom. Lett.*, early access, Feb. 25, 2021, doi: 10.1109/LRA.2021.3062336.
- [41] M. A. Oskoei and H. Hu, "Support vector machine-based classification scheme for myoelectric control applied to upper limb," *IEEE Trans. Biomed. Eng.*, vol. 55, no. 8, pp. 1956–1965, Aug. 2008.
- [42] Z. Wu and X. Li, "A wireless surface EMG acquisition and gesture recognition system," in *Proc. 9th Int. Congr. Image Signal Process., Biomed. Eng. Informat. (CISP-BMEI)*, Oct. 2016, pp. 1675–1679.
- [43] K. Englehart and B. Hudgins, "A robust, real-time control scheme for multifunction myoelectric control," *IEEE Trans. Biomed. Eng.*, vol. 50, no. 7, pp. 848–854, Jul. 2003.
- [44] H. Zhang, Y. Zhao, F. Yao, L. Xu, P. Shang, and G. Li, "An adaptation strategy of using LDA classifier for EMG pattern recognition," in *Proc. 35th Annu. Int. Conf. IEEE Eng. Med. Biol. Soc. (EMBC)*, Jul. 2013, pp. 4267–4270.
- [45] M. Atzori, A. Gijsberts, H. Muller, and B. Caputo, "Classification of hand movements in amputated subjects by sEMG and accelerometers," in *Proc. 36th Annu. Int. Conf. IEEE Eng. Med. Biol. Soc.*, Aug. 2014, pp. 3545–3549.
- [46] R. A. R. Chand, K. Kiguchi, R. A. R. C. Gopura, and K. Kiguchi, "An exoskeleton robot for human forearm and wrist motion assist," *J. Adv. Mech. Des. Syst. Manuf.*, vol. 2, no. 6, pp. 1067–1083, 2008.
- [47] S. Benatti, F. Casamassima, B. Milosevic, E. Farella, P. Schönle, S. Fateh, T. Burger, Q. Huang, and L. Benini, "A versatile embedded platform for EMG acquisition and gesture recognition," *IEEE Trans. Biomed. Circuits Syst.*, vol. 9, no. 5, pp. 620–630, Oct. 2015.
- [48] M. A. Waris, M. Jamil, Y. Ayaz, and S. O. Gilani, "Classification of functional motions of hand for upper limb prosthesis with surface electromyography," *Int. J. Biol. Biomed. Eng.*, vol. 8, pp. 15–20, Jan. 2014.
- [49] X. Zhang and P. Zhou, "Classification of upper limb motions in stroke using high density surface EMG," in *Proc. Annu. Int. Conf. IEEE Eng. Med. Biol. Soc.*, Aug. 2011, pp. 3367–3370.
- [50] J. Liu and P. Zhou, "A novel myoelectric pattern recognition strategy for hand function restoration after incomplete cervical spinal cord injury," *IEEE Trans. Neural Syst. Rehabil. Eng.*, vol. 21, no. 1, pp. 96–103, Jan. 2013.
- [51] J. G. Ngeo, T. Tamei, and T. Shibata, "Continuous and simultaneous estimation of finger kinematics using inputs from an EMG-to-muscle activation model," *J. NeuroEng. Rehabil.*, vol. 11, no. 1, pp. 1–14, Dec. 2014.
- [52] B. Guo, Y. Ma, J. Yang, Z. Wang, and X. Zhang, "Lw-CNN-based myoelectric signal recognition and real-time control of robotic arm for upper-limb rehabilitation," *Comput. Intell. Neurosci.*, vol. 2020, pp. 1–12, Dec. 2020.
- [53] N. Secciani, A. Topini, A. Ridolfi, E. Meli, and B. Allotta, "A novel point-in-polygon-based sEMG classifier for hand exoskeleton systems," *IEEE Trans. Neural Syst. Rehabil. Eng.*, vol. 28, no. 2, pp. 3158–3166, Dec. 2020.
- [54] S. Ueki, H. Kawasaki, S. Ito, Y. Nishimoto, N. Abe, T. Aoki, Y. Ishigure, T. Ojika, and T. Mouri, "Development of a hand-assist robot with multi-degrees-of-freedom for rehabilitation therapy," *IEEE/ASME Trans. Mechatronics*, vol. 17, no. 1, pp. 136–146, Feb. 2012.
- [55] N. Hajializade, M. Abdolvahab, H. Bagheri, M. Jalili, A. Baghestani, E. Entezari, and M. Mandegari, "The effect of task-based mirror therapy on upper limb functions and activities of daily living in patients with chronic cerebrovascular accident: A randomized control trial," *J. Basic Clin. Pathophysiol.*, vol. 1, no. 1, pp. 1–12, 2016.
- [56] H. Thieme, N. Morkisch, J. Mehrholz, M. Pohl, J. Behrens, B. Borgetto, and C. Dohle, "Mirror therapy for improving motor function after stroke," *Cochrane Database Syst. Rev.*, vol. 7, no. 7, pp. 1–154, 2018.
- [57] D. Leonardis, M. Barsotti, C. Loconsole, M. Solazzi, M. Troncosi, C. Mazzotti, V. P. Castelli, C. Procopio, G. Lamola, C. Chisari, and M. Bergamasco, "An EMG-controlled robotic hand exoskeleton for bilateral rehabilitation," *IEEE Trans. Haptics*, vol. 8, no. 2, pp. 140–151, Jun. 2015.
- [58] H. Wu, J. Liu, H. Handroos, B. Miraftehi, A. Heinonen, S. Peurala, I. Tarkka, M. Rossi, and S. Nousiainen, "Virtual reality based robotic therapy for stroke rehabilitation: An initial study," in *Proc. IEEE Int. Conf. Mechatronics Autom.*, Aug. 2011, pp. 1196–1200.
- [59] H. Nakayama, H. S. Jørgensen, H. O. Raaschou, and T. S. Olsen, "Recovery of upper extremity function in stroke patients: The Copenhagen stroke study," *Arch. Phys. Med. Rehabil.*, vol. 75, no. 4, pp. 394–398, Apr. 1994.
- [60] X. L. Hu, K. Y. Tong, X. J. Wei, W. Rong, E. A. Susanto, and S. K. Ho, "The effects of post-stroke upper-limb training with an electromyography (EMG)-driven hand robot," *J. Electromyogr. Kinesiol.*, vol. 23, no. 5, pp. 1065–1074, 2013.
- [61] J. M. Ochoa, Y. Jia, D. Narasimhan, and D. G. Kamper, "Development of a portable actuated orthotic glove to facilitate gross extension of the digits for therapeutic training after stroke," in *Proc. Annu. Int. Conf. IEEE Eng. Med. Biol. Soc.*, Sep. 2009, pp. 6918–6921.
- [62] R. Riener and M. Munih, "Guest editorial special section on rehabilitation via bio-cooperative control," *IEEE Trans. Neural Syst. Rehabil. Eng.*, vol. 18, no. 4, pp. 337–338, Aug. 2010.
- [63] Y. Muraoka, A. Ishio, and K. Takeda, "Low-cost 2ch EMG biofeedback device using a stereo microphone port," *Jpn. J. Compr. Rehabil. Sci.*, vol. 5, pp. 1–6, Jan. 2014.
- [64] S. Benatti, B. Milosevic, F. Casamassima, P. Schonle, P. Bunjaku, S. Fateh, Q. Huang, and L. Benini, "EMG-based hand gesture recognition with flexible analog front end," in *Proc. IEEE Biomed. Circuits Syst. Conf. (BioCAS)*, Oct. 2014, pp. 57–60.
- [65] F. Tenore, R. S. Armiger, R. Jacob Vogelstein, D. S. Wenstrand, S. D. Harshbarger, and K. Englehart, "An embedded controller for a 7-degree of freedom prosthetic arm," in *Proc. 30th Annu. Int. Conf. IEEE Eng. Med. Biol. Soc.*, Aug. 2008, pp. 185–188.
- [66] J. Liu, F. Zhang, and H. H. Huang, "An open and configurable embedded system for EMG pattern recognition implementation for artificial arms," in *Proc. 36th Annu. Int. Conf. IEEE Eng. Med. Biol. Soc.*, Aug. 2014, pp. 4095–4098.

- [67] D. Brunelli, E. Farella, D. Giovannelli, B. Milosevic, and I. Minakov, "Design considerations for wireless acquisition of multichannel sEMG signals in prosthetic hand control," *IEEE Sensors J.*, vol. 16, no. 23, pp. 8338–8347, Dec. 2016.
- [68] I. B. Abdallah, Y. Bouteraa, and C. Rekek, "Design and development of 3D printed myoelectric robotic exoskeleton for hand rehabilitation," *Int. J. Smart Sens. Intell. Syst.*, vol. 10, no. 2, pp. 341–366, 2017.
- [69] Z. Lu, X. Chen, X. Zhang, K. Y. Tong, and P. Zhou, "Real-time control of an exoskeleton hand robot with myoelectric pattern recognition," *Int. J. Neural Syst.*, vol. 27, no. 5, pp. 1–11, 2017.
- [70] J. Zhang, B. Wang, C. Zhang, Y. Xiao, and M. Y. Wang, "An EEG/EMG/EOG-based multimodal human-machine interface to real-time control of a soft robot hand," *Frontiers Neurobot.*, vol. 13, p. 7, Mar. 2019.
- [71] S. Park, M. Fraser, L. M. Weber, C. Meeker, L. Bishop, D. Geller, J. Stein, and M. Ciocarlie, "User-driven functional movement training with a wearable hand robot after stroke," *IEEE Trans. Neural Syst. Rehabil. Eng.*, vol. 28, no. 10, pp. 2265–2275, Oct. 2020.
- [72] M. K. Burns, D. Pei, and R. Vinjamuri, "Myoelectric control of a soft hand exoskeleton using kinematic synergies," *IEEE Trans. Biomed. Circuits Syst.*, vol. 13, no. 6, pp. 1351–1361, Dec. 2019.
- [73] S. Park, C. Meeker, L. M. Weber, L. Bishop, J. Stein, and M. Ciocarlie, "Multimodal sensing and interaction for a robotic hand orthosis," *IEEE Robot. Autom. Lett.*, vol. 4, no. 2, pp. 315–322, Apr. 2019.
- [74] Y. Chen, Z. Yang, and Y. Wen, "A soft exoskeleton glove for hand bilateral training via surface EMG," *Sensors*, vol. 21, no. 2, pp. 1–18, 2021.
- [75] F. Montagnani, M. Controzzi, and C. Cipriani, "Independent long fingers are not essential for a grasping hand," *Sci. Rep.*, vol. 6, no. 1, pp. 1–9, Dec. 2016.
- [76] V. Moreno-SanJuan, A. Cisnal, J.-C. Fraile, J. Pérez-Turiel, and E. de-la-Fuente, "Design and characterization of a lightweight underactuated RACA hand exoskeleton for neurorehabilitation," *Robot. Auto. Syst.*, vol. 143, Sep. 2021, Art. no. 103828.
- [77] S. Cobos, M. Ferre, M. A. S. Uran, J. Ortego, and C. Pena, "Efficient human hand kinematics for manipulation tasks," in *Proc. IEEE/RSSJ Int. Conf. Intell. Robots Syst.*, Sep. 2008, pp. 2246–2251.
- [78] SENIAM. Accessed: Feb. 19, 2021. [Online]. Available: <http://www.seniam.org>
- [79] M. Halaki and K. Ginn, "Normalization of EMG signals: To normalize or not to normalize and what to normalize," in *Computational Intelligence in Electromyography Analysis—A perspective on Current Applications and Future Challenges*, G. Naik, Ed. Rijeka, Croatia: InTech, 2012, pp. 175–194.
- [80] R. H. Chowdhury, M. B. I. Reaz, M. A. B. M. Ali, A. A. A. Bakar, K. Chellappan, and T. G. Chang, "Surface electromyography signal processing and classification techniques," *Sensors*, vol. 13, no. 9, pp. 12431–12466, 2013.
- [81] E. Yang and M. C. Dorneich, "The effect of time delay on emotion, arousal, and satisfaction in human-robot interaction," in *Proc. Hum. Factors Ergon. Soc. 59th Annu. Meeting*, vol. 2015, pp. 443–447.
- [82] G. Li, A. E. Schultz, and T. A. Kuiken, "Quantifying pattern recognition—Based myoelectric control of multifunctional transradial prostheses," *IEEE Trans. Neural Syst. Rehabil. Eng.*, vol. 18, no. 2, pp. 185–192, Apr. 2010.
- [83] T. R. Farrell and R. F. Weir, "The optimal controller delay for myoelectric prostheses," *IEEE Trans. Neural Syst. Rehabil. Eng.*, vol. 15, no. 1, pp. 111–118, Mar. 2007.
- [84] S. Tam, M. Boukadoum, A. Campeau-Lecours, and B. Gosselin, "A fully embedded adaptive real-time hand gesture classifier leveraging HD-sEMG and deep learning," *IEEE Trans. Biomed. Circuits Syst.*, vol. 14, no. 2, pp. 232–243, Apr. 2020.
- [85] Y. Hu, Z. Li, G. Li, P. Yuan, and C. Yang, "Development of sensory-motor fusion-based manipulation and grasping control for a robotic hand-eye system," *IEEE Trans. Syst. Man Cybern. Syst.*, vol. 47, no. 7, pp. 1169–1180, Jul. 2017.
- [86] V. H. Cene and A. Balbinot, "Resilient EMG classification to enable reliable upper-limb movement intent detection," *IEEE Trans. Neural Syst. Rehabil. Eng.*, vol. 28, no. 11, pp. 2507–2514, Nov. 2020.
- [87] F. Ryser, T. Butzer, J. P. Held, O. Lamberg, and R. Gassert, "Fully embedded myoelectric control for a wearable robotic hand orthosis," in *Proc. Int. Conf. Rehabil. Robot. (ICORR)*, Jul. 2017, pp. 615–621.
- [88] J.-U. Chu, I. Moon, and M.-S. Mun, "A real-time EMG pattern recognition system based on linear-nonlinear feature projection for a multi-function myoelectric hand," *IEEE Trans. Biomed. Eng.*, vol. 53, no. 11, pp. 2232–2239, Nov. 2006.



ANA CISNAL (Student Member, IEEE) received the B.S. degree in industrial electronics and automation engineering and the M.S. degree in industrial engineering from the University of Valladolid, Valladolid, Spain, in 2017 and 2019, respectively, where she is currently pursuing the Ph.D. degree in industrial engineering.

During 2016, she has participated in quality internships at the Technology Center CARTIF, Valladolid, and Fraunhofer IBMT, Sankt Ingbert, Germany. Since 2017, she has been working at the Advanced Production Technologies Institute (ITAP), University of Valladolid, as a Research Fellow and a Contract Researcher. Her current research interest includes development of control strategies for bio-cooperative controls for robotic neuromotor rehabilitation platforms. She became a Student Member, in 2018.



JAVIER PÉREZ-TURIEL received the Ph.D. degree in control engineering from the University of Valladolid, Spain, in 1994.

In 1999, he was a Visiting Professor at the Electrical Engineering and Computer Science Department (EECS), University of Michigan, USA. He was the Head of the Biomedical Engineering Division, CARTIF Technological Center, from 2000 to 2014. He is a member of the Medical Robotics Group, Institute of Advanced Production Technologies (ITAP) University Institute. He is currently an Associate Professor at the Department of Systems Engineering, University of Valladolid. His research interests include surgical and rehabilitation robots.



JUAN-CARLOS FRAILE received the Ph.D. degree in control engineering from the Faculty of Engineering, University of Valladolid, Spain, in 1987. Since 1992, he has been an Associate Professor of control and robotics with the Faculty of Engineering, University of Valladolid. In 1998, he was a Visiting Professor in engineering systems at the Institute of Complex Engineering Systems (ICES), Carnegie Mellon University, Pittsburgh, USA. He is the Leader of the ITAP-Medical Robotics Group, University of Valladolid. His current research interests include rehabilitation robotics and robots for surgery.



DAVID SIERRA was born in Salamanca, Spain, in 1996. He received the B.S. degree in industrial electronics and automation engineering from the University of Valladolid, Valladolid, Spain, in 2019. In 2018, he had an internship at the Hospital del Mar, Barcelona, Spain. Since 2019, he has been working at the Institute of Advanced Production Technologies, Valladolid University, as a Research Fellow and a Contract Researcher. His current research interests include development of virtual reality environments and augmented reality for upper-limb neuromotor rehabilitation.



EUSEBIO DE LA FUENTE received the M.Sc. degree in electronic engineering and automatic control and the Ph.D. degree from the University of Valladolid, Spain, in 1991 and 1997, respectively. Since 1999, he has been an Associate Professor in computer science with a specialization in computer vision at the Industrial Engineering School, Valladolid, Spain. His current research interests include the field of medical image processing and real-time video analysis for rehabilitation and surgical robot applications. He is especially interested in deep learning techniques for object detection in medical images and classification.